Graphene

Graphene and artificial graphene

Marco Polini

m.polini@sns.it

Collaborators
G. Borghi
F. Dolcini
R. Fazio
M. Gibertini
B. Karmakar
V. Pellegrini
S. Peotta
A. Principi
D. Rainis
A. Singha
F. Taddei
A. Tomadin

This area of research focuses on a novel class of two-dimensional (2D) electron liquids subjected to a lateral potential of honeycomb symmetry. During the years 2004-2005 a group in Europe (A. Geim and co-workers at the University of Manchester, UK) and one in the US (P. Kim and co-workers at the Columbia University, USA) have succeeded in the isolation of single- and few-layer ìgrapheneî systems (see below) from graphite. Electrons in doped single-layer graphene behave like massless fermions. Graphene is a first remarkable and clean example of the impact of a potential with honeycomb structure on the electronic states and dynamics. In graphene the crystalline potential is determined by the spatial arrangement of Carbon atoms leading to linearly dispersing Dirac-cone bands and semimetallic behavior. When Coulombic electron-electron interactions are included, doped graphene represents a new type of many-electron problem, distinct from both an ordinary 2D electron gas and from quantum electrodynamics. Below we summarize some of the theoretical work done in this area of research. We also show that linearly-dispersing bands and massless-Dirac-fermion behavior can be induced in an ordinary 2D electron gas in GaAs/AlGaAs heterostructures when subjected to an external lateral potential with honeycomb symmetry that can be realized e.g. by nanofabrication.

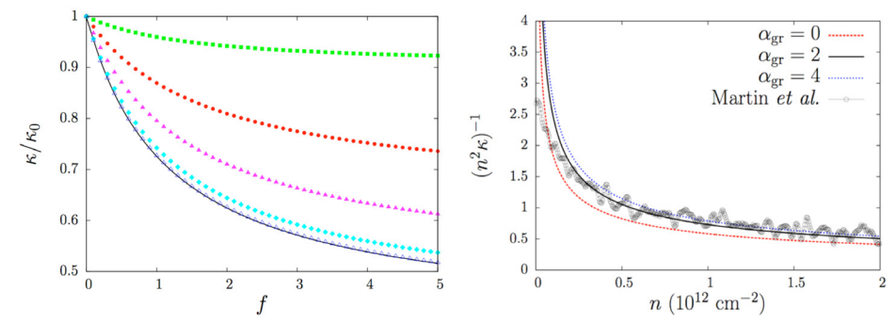

Fig. 1
(Left panel) The ratio between the compressibility of an interacting doped graphene sheet and the corresponding quantity for the noninteracting system is plotted as a function of graphene's fine-structure constant. The various curves refer to different values of density: from top to bottom density decreases. Note that interactions suppress the compressibility rather than enhancing it. The chiral nature of low-energy electrons in graphene is at the origin of this unusual many-body effect [2]. (Right panel) The thermodynamical density-of-states as a function of electron density. The theoretical results of Ref. [2] (solid lines, referring to different values of the fine-structure coupling constant) are compared with the experimental results of Ref. [8] (empty circles).

Electron-electron interactions in doped graphene sheets

Graphene is a one-atom-thick electron system composed of Carbon atoms on a 2D honeycomb lattice, which has attracted an exceptional amount of interest in the scientific community [1]. We have investigated the interplay between chirality and electron-electron interactions in determining thermodynamic quantities (such as compressibility - see Fig. 1 - and spin susceptibility) of doped graphene sheets [2]. We have also studied one-particle properties, carrying out calculations of the velocity renormalization [3], of the quasiparticle self-energy [3,4], and of the quasiparticle spectral function [4] (see Fig. 2). Similar studies have been carried out at finite temperature [5] and for bilayer graphene [6]. Finally, we have

also developed a Kohn-Sham-Dirac self-consistent scheme for graphene sheets that treats slowly-varying inhomogeneous external potentials and electron-electron interactions on an equal footing [7] (see Fig. 3).

Pseudospintronics with semiconductor and graphene bilayers

The layer degree-of-freedom in semiconductor quantum wells and in graphene bilayers can be viewed as a spin-1/2-like quantum degree-of-freedom. In particular this ìpseudospinî quantum number gives rise to a collective mode analogous to the ferromagnetic resonance mode of a ferromagnet. In Ref. [9] we have outlined a many-body theory of the dependence of the energy and the damping of this mode on layer separation. Based on these results, we have discussed the possibilities of realizing transport-current driven pseudospin-transfer oscillators in semiconductors, and of using the pseudospin-transfer effect as an experimental probe of intersubband plasmons. In Ref. [10] we have predicted that neutral graphene bilayers are pseudospin magnets in which the charge density-contribution from each valley and spin spontaneously shifts to one of the two layers. The band structure of this system is characterized by a momentum-space vortex, which is responsible for unusual competition between band and kinetic energies leading to symmetry breaking in the vortex core. We have also discussed the possibility of realizing a pseudospin version of ferromagnetic metal spintronics in graphene bilayers based on hysteresis associated with this broken symmetry.

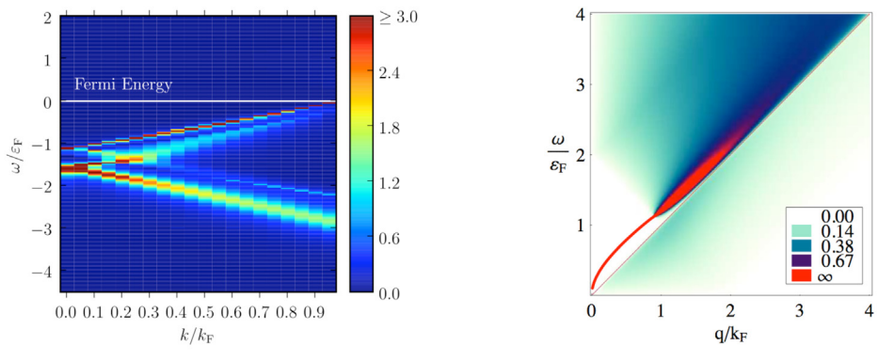

Fig. 2
(Left panel) A color plot of the spectral function of a n-doped graphene sheet as a function of momentum and energy [4]. For each value of momentum angle-resolved photoemission spectroscopy (ARPES) detects the portion of the spectral function with negative energy. The negative-energy ARPES spectra of a p-doped graphene sheet is identical to the positive-energy spectra of an n-doped sheet. (Right panel) The imaginary part of the inverse dielectric function is plotted as a function of momentum and energy. The plasmon collective mode is represented by the red line: it remains remarkably well defined even when it enters the interband electron-hole continuum.

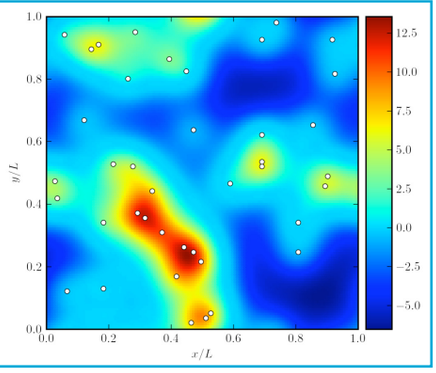

Fig. 3
A color plot of the Kohn-Sham-Dirac [5] self-consistent ground-state density profile of a 2D system of interacting massless Dirac fermions in the presence of fourty randomly-distributed Coulomb impurities (white circles) located away from the graphene plane. This particular result corresponds to a neutral-on-average graphene sheet. The ground-state density profile of weakly-doped graphene sheets is highly inhomogeneous, due to the random potential landscape created by the impurities, and is characterized by electron- and hole-rich puddles.

Transport in hybrid graphene/superconductor junction

We have studied Andreev reflection in graphene nanoribbon/superconductor hybrid junctions [11]. By using a tight-binding approach and the scattering formalism we have shown that finite-size effects lead to notable differences with respect to the bulk graphene case. At subgap voltages, conservation of *pseudoparity*, a quantum number characterizing the ribbon states, yields either a suppression of Andreev reflection when the ribbon has an even number of sites in the transverse direction or perfect Andreev reflection when the ribbon has an odd number of sites. In the former case the suppression of Andreev reflection induces an insulating behavior even when the junction is biased; electron conduction can however be restored by applying a gate voltage. Finally, we have also checked that these findings remain valid in the case of *nonideal* nanoribbons in which the number of transverse sites varies along the transport direction.

Dirac fermions in Gallium Arsenide: artificial graphene

In the following we report on the fabrication of a device from semiconducting heterostructures that has the potential to behave like graphene [12]. The starting material is a two-dimensional electron gas of very high purity confined in an AlGaAs/GaAs modulation-doped quantum well. On top of this, a honeycomb network of nanosized ìpillarsî analogous to carbon ions in the graphene lattice, modulates the electric potential in the two-dimensional electron gas. A SEM image of a typical sample is shown in Fig. 4 (left panel). The same figure shows (right panel) the calculated energy minibands for a muffin-tin potential with such honeycomb symmetry with the experimental parameters *a=150* nm, *r= 52.5* nm, and with a chosen V_0 = -0.8 meV, where V_0 is the estimated strength of attractive potential experienced by the electrons in the nanosized regions of diameter *2r=105* nm.

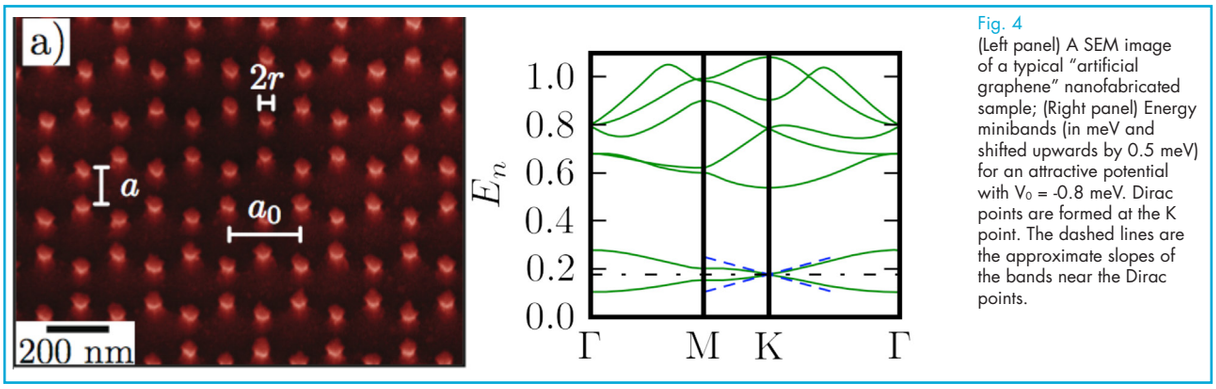

Fig. 4
(Left panel) A SEM image of a typical "artificial graphene" nanofabricated sample; (Right panel) Energy minibands (in meV and shifted upwards by 0.5 meV) for an attractive potential with V_0 = -0.8 meV. Dirac points are formed at the K point. The dashed lines are the approximate slopes of the bands near the Dirac points.

As dictated by symmetry and group theory, these minibands are characterized by the existence of two-fold degenerate points at the corners of the Brillouin zone. It is easy to show that states close to these points are effectively described by a two-component massless Dirac fermion Hamiltonian.

Figure 5 shows representative photoluminescence (PL) spectra at 2K both of the unprocessed (red dotted curve) and processed (black solid curve) samples. In the unprocessed 2DEG case, the PL shape is determined by the density-of-states of the free electrons and equilibrium occupation factors of the 2DEG and photoexcited holes leading to an estimated electron density of around 10^{11} cm^{-2} in agreement with the transport results. The processed sample PL, on the contrary, displays a re-

markable change with the appearance of sharp structures on the high-energy side and an overall reduction of its linewidth, which are consistent with the modification of the conventional constant-in-energy DOS as shown in Fig. 5, provided that V_0 is chosen appropriately (V_0 = -2.8 meV in this plot). The overall smaller linewidth of the PL suggests a reduction of the average electron density due to the impact of the etching process. Work is in progress to study the evolution of the cyclotron resonance in a magnetic field.

Fig. 5
Panel a) Calculated density-of-states (DOS), in units of $eV^{-1}nm^{-2}$, as a function of energy for a muffin-tin potential with V_0 = -2.8 meV, a=150 nm, and r=52.5 nm. The first structure in the DOS is fixed at the energy of the main photoluminescence (PL) peak (see panel b). The vertical dashed line denotes the Fermi level associated with the nominal density of 1.1×10^{11} cm^{-2}. The insets to Fig. 5a show the Brillouin zone corresponding to the external periodic potential and a zoom of the DOS corresponding to the first structure in the main panel. The V-shaped DOS characteristic of MDFs is evident. Panel b) Low-temperature (T=2 K) PL of the sample before (red dotted curve) and after (black solid curve) the processing.

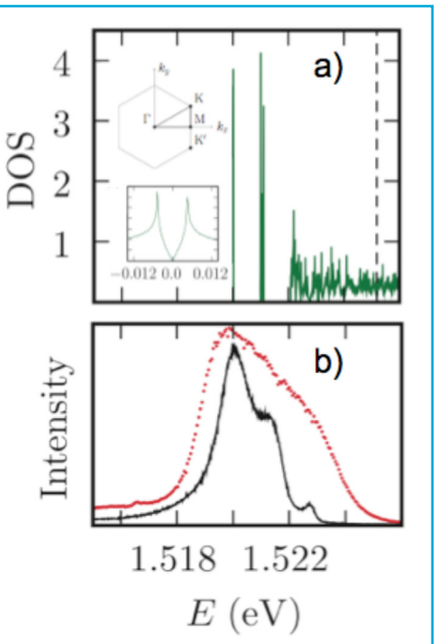

Such artificially engineered ìgrapheneî may offer some advantages over its natural prototype, such as extremely high purity of samples, an ability to tune the parameters of the spectrum, and the possibility of shaping the artificial graphene into geometries like ribbons with perfect edges, which are more useful in certain applications.

References

[1] A.H. Castro Neto *et al.*, Rev. Mod. Phys. 81, 109 (2009); A.K. Geim and A.H. MacDonald, Phys. Today 60 (8), 35 (2007); A.K. Geim and K.S. Novoselov, Nature Mater. 6, 183 (2007).
[2] Y. Barlas *et al.*, Phys. Rev. Lett. 98, 236601 (2007).
[3] M. Polini *et al.*, Solid State Commun. 143, 58 (2007).
[4] M. Polini *et al.*, Phys. Rev. B 77, 081411(R) (2008).
[5] M.R. Ramezanali *et al.*, J. Phys. A: Math. Theor. 42, 214015 (2009).
[6] G. Borghi *et al.*, Solid State Commun. 149, 1117 (2009).
[7] M. Polini *et al.*, Phys. Rev. B 78, 115426 (2008); see also A. Principi, M. Polini, and G. Vignale, Phys. Rev. B 80, 075418 (2009).
[8] J. Martin *et al.*, Nature Phys. 4, 144 (2008).
[9] S.H. Abedinpour *et al.*, Phys. Rev. Lett. 99, 206802 (2007).
[10] H. Min *et al.*, Phys. Rev. B 77, 041407(R) (2008).
[11] D. Rainis *et al.*, Phys. Rev. B 79, 115131 (2009).
[12] M. Gibertini *et al.*, Phys. Rev. B 79, 241406(R) (2009).